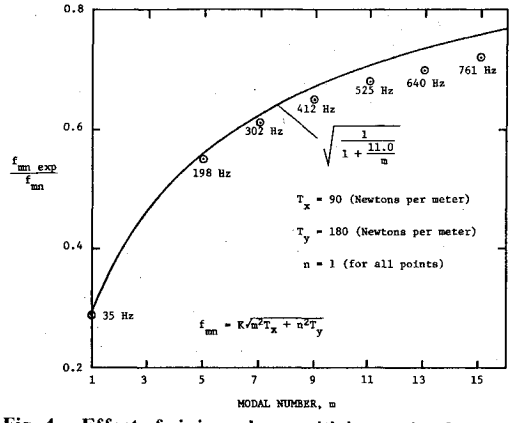

Fig. 4 Effect of air impedance with increasing frequency.

Eq. (2) in the case in which $n=1$ and m is varied form 1 to 15. Assuming that the factor K in Eq. (2) can be corrected for air impedance by writing

$$K' = 1/2\sqrt{(M+M_a)}$$

where M is the mass of the membrane and M_a is the effective added mass of air, the frequency ratio shown is expressible as K'/K where

$$K'/K = \sqrt{M/(M+M_a)}$$

If the added mass is assumed to be proportional to the wavelength λ of the standing wave, where $\lambda = 2a/m$, then

$$K'/K = 1/\sqrt{1+c/m} \tag{3}$$

where c is a constant. Matching this expression to the experimentally determined frequency ratio for $m=1$, the value of c is found to be 11.0. Equation (3), as shown in Fig. 4, is in reasonable agreement with the trend of the measured frequency ratios.

References

[1] Blick, E.F., Walters, R. R., and Smith, R., "Compliant Coating Skin Friction Experiments," AIAA Paper 69-165, New York, 1969.

[2] Lissaman, P. B. S. and Harris, G. L., "Turbulent Skin Friction on Compliant Surfaces," AIAA Paper 69-164, New York, 1969.

[3] McAlister, K. W. and Wynn, T.M., "Experimental Evaluation of Compliant Surfaces at Low Speeds," NASA TM X-3119, 1974.

[4] Ash, R. L. and Bushnell, D. M., "Compliant Wall Turbulent Skin-Friction Reduction Research," AIAA Paper 75-833, 1975.

[5] Morse, P. M., *"Vibration and Sound,"* McGraw-Hill, New York 1948, pp. 332-333.

Anisotropic Radiatively Coupled Wedge Flow

James B. Elgin* and Judson R. Baron†
Massachusetts Institute of Technology, Cambridge, Mass.

Introduction

GEOMETRICALLY thin shock layers are advantageous in reducing the radiation heat transfer to a high-speed body. Gibeling and one of the present authors[1] have shown, in fact, that optimum two-dimensional bodies for minimizing the overall radiant heat transfer correspond closely to those associated with reductions in the disturbed volume of air when the field is radiatively coupled. However, elongated shock layers imply anisotropic radiation fields. Therefore, the differential [Milne-Eddington (*M.E.*)] approximation used in Ref. 1 is somewhat questionable.

In the optically thin limit for which emission dominates and reabsorption is negligible, a purely differential description is appropriate. Wedge flow results have been carried out for that limit by Jischke[2] using an integral method, and Olfe[3] based on an expansion in shock density ratio.

Recently, an extension of the Milne-Eddington has been proposed and evaluated.[4,5] The essential improvement was the introduction of variable closure for the higher moments of the intensity distribution (or equivalently for a higher-order spherical harmonics expansion) based on ellipsoidal intensity distribution modeling. The inadequacy of *M.E.* to represent anisotropic radiation fields was shown there by means of comparisons of exact, variable closure, and *M.E.* evaluations for several representative regions. These included quite thin (10°-170°) rhombic section prisms, and concentric annular regions between cylinders and cones, all being representative of shock-layer regions. Geometric corners imply a most severe test for radiative approximations of a differential nature. *M.E.* showed marked departures from the exact values for flux and intensity in such regions, but the variable closure ellipsoids gave rather good agreement. This suggests the utility of ellipsoidal modeling for both anisotropic and coupled fields. The purpose here is an application of the concept to a radiatively coupled wedge flow, which is a reference case considered in Ref. 1 and provides a realistic basis for examination of *M.E.* adequacy for shock layers.

Analysis

The fluid field is specified by an integral method and, consistent with this, the radiation intensity is specified by an assumed distribution across the shock layer. For an inviscid, perfect-gas continuum, the radiation contribution to the fluid field description[6,7] is the nonadiabatic flux divergence term

$$\nabla \cdot \bar{q} = \alpha(4\sigma T^4 - I_0) \tag{1}$$

in the energy balance. Here, α is a temperature-dependent grey gas absorption coefficient[5] and I_0 is the zeroth angular moment of intensity, i.e., $\int_{4\pi} I d\Omega$. Significantly, only the lowest order moment is required explicitly since the absorption process is independent of the photon direction of travel through a point.

Although coupled to the fluid field, it proves convenient to consider I_0 as a parametric function of the problem and proceed iteratively based on an initial assumption of $I_0 \equiv 0$. The physical rationale is an increasing absorption with successive iteration cycles. Since the energy loss from each fluid element during a given cycle is greater than would be expected with full reabsorption, the temperature level for each cycle is too small. Corresponding radiation moments then are based on lower emission levels and a uniformly lower I_0 increases monotonically with iteration cycle. The essential advantage is a separation of radiation and fluid-field evaluations; the adequacy of the converged solution depends upon the accuracy of the basis for I_0.

Since field points located away from the boundaries are irradiated over relatively larger solid angles, an I_0 maximum is to be anticipated between the surface and shock. Assuming a parabolic distribution of the form

$$I_0(x,y) = I_{0_0}(x) + I_{0_1}(x)(y/\delta) + I_{0_2}(x)(y/\delta)^2 \tag{2}$$

implies the need for I_0 at $y=0$, $(\delta/2)$, and δ; i.e., in Eq. (2)

$$I_{0_i} = a_i I_0(x,0) + b_i I_0[x,(\delta/2)] + c_i I_0(x,\delta) \tag{3}$$

Received May 20, 1976. Supported by the U.S. Air Force Office of Scientific Research under Contract F44620-75-C-0040.

Index categories: Radiatively Coupled Flows and Heat Transfer; Radiation and Radiative Heat Transfer; Supersonic and Hypersonic Flow.

*Research Assistant. Presently at Aerodyne Research, Inc., Bedford, Mass.

†Professor, Department of Aeronautics and Astronautics.

with $(a_i,b_i,c_i)=(1,0,0)$, $(-3,4,-1)$, $(2,-4,2)$ for $i=0,1,2$, respectively.

The introduction of ellipsoidal modeling for the specific intensity distribution implies a need for only relatively coarse subdivisions. The present approach with I_0 as a lagging nonadiabatic parameter requires a systematic specification of the elliptic sections for a given fluid field. Conceptually, however, the variable closure ellipsoids provide for a more accurate representation of the higher moments for the field intensity.[4,5]

Consider a unit vector, i_s, in an arbitrary s direction with direction cosines $(\ell_x,\ell_y,\ell_z)=(\sin\theta\cos\phi, \sin\theta\sin\phi, \cos\theta)$ relative to a surface-aligned (x,y,z) coordinate system as in Fig. 1a. The intensity follows from integration of the transfer relation

$$(dI/ds)=\alpha[(\sigma T^4/\pi)-I] \tag{4}$$

and for both $\theta=0$ and π, $I=\sigma T^4/\pi(=I_b$, say). Assuming an elliptical variation in intensity in a given ϕ plane,

$$I(\theta,\phi)=\mathcal{I}(\phi)I_b/\sqrt{(I_b\sin\theta)^2+[\mathcal{I}(\phi)\cos\theta]^2} \tag{5}$$

where $\mathcal{I}(\phi)\equiv I(\pi/2,\phi)$. The general intensity moments are then

$$I_{ij}=\int_{4\pi} I\,\ell_x^i\ell_y^j d\Omega=2\int_0^{2\pi}\cos^i\phi\sin^j\phi H[I_b,\mathcal{I}(\phi),i+j+1]d\phi \tag{6}$$

in terms of $\mathcal{I}(\phi)$, modeling and the function[5]

$$H[A,B,n]=AB\int_0^{\pi/2}\sin^n\xi d\xi/\sqrt{(A\sin\xi)^2+(B\cos\xi)^2} \tag{7}$$

The remaining $\theta=\pi/2$ section model follows from a consideration of the characteristic ϕ_i angles to the three shock-layer corners (Fig. 1c), i.e.,

$$(\phi_1,\phi_2,\phi_3)=\left\{\left[\tan^{-1}\frac{y}{x}\right],\left[\frac{\pi}{2}+\tan^{-1}\left(\frac{1-x}{y}\right)\right],\left[\pi+\tan^{-1}\frac{\delta(1)-y}{1-x}\right]\right\} \tag{8}$$

It must be anticipated that discontinuous angular derivatives of intensity will be present along such ϕ_i rays, and the inherent segmentation is of some importance for realistic modeling. Integration of Eq. (4) along the boundaries and bisectors [ϕ_i and $(\phi_1+\phi_2)/2$, etc.] of the three naturally defined plane regions follows with the use of α, T, and δ from the previous fluid field. For any angle pair, ϕ_i, ϕ_j, and their corresponding intensities, $I_i\geq I_j$, say, an elliptic section may be constructed with the major axis aligned along ϕ_i and the axes ratio adjusted to fit the intensities. Thus

$$\mathcal{I}(\phi)=I_iI_l/\sqrt{[I_i\sin(\phi-\phi_i)]^2+[I_l\cos(\phi-\phi_i)]^2} \tag{9}$$

in which

$$I_l=I_iI_j|\sin(\phi_j-\phi_i)|/\sqrt{I_i^2-[I_j\cos(\phi_j-\phi_i)]^2} \tag{10}$$

This representation is useful for interior points within all six angular segments. For surface and downstream boundary points, the intensity sections corresponding to emerging radiation vanish appropriately. The somewhat artificial downstream boundary is introduced as a simplification. The neglected downstream layer continues to radiate until eventually cooled by trailing-edge expansion processes; its omission appears justified by the negligibly small solid angle subtended in cases involving geometrically thin layers. Any appreciable influence is confined to a region on the order of several layer thicknesses upstream of the trailing edge.

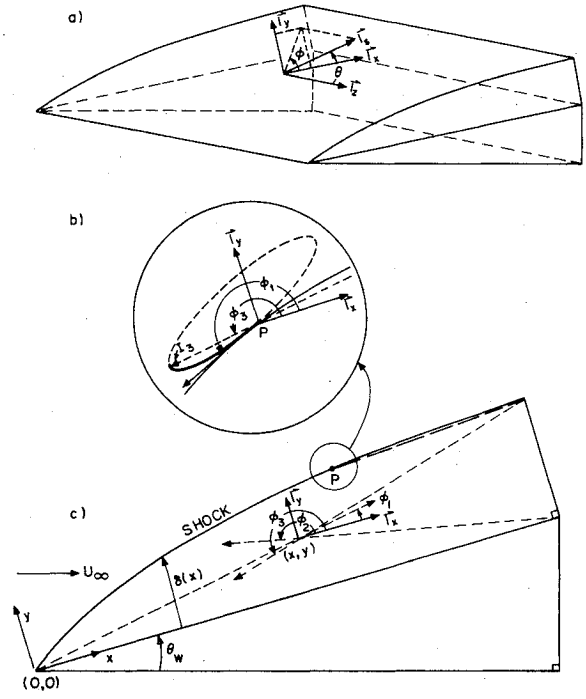

Fig. 1 Wedge field geometry.

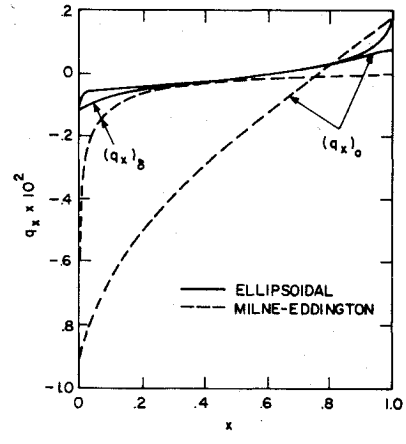

Fig. 2 Flux distributions parallel to surface, along surface and shock. $\theta_w=0.61$ rad, $(M_\infty,\tau_L,Bo)=(28.5, 0.62, 0.027)$.

At a shock boundary point, the shock curvature introduces a solid angle over which the shock is viewed (Fig. 1b). The intensity vanishes as ϕ approaches coincidence with the shock tangent, and the maximum intensity generally corresponds to the longest radiating path length, either ϕ_1 or ϕ_3. This suggests a tangent ellipse model. If ϕ_t locates the shock tangent, and ϕ_k, I_k refer to the $k=1$ or 3 direction values, then for the shock viewed segment

$$\mathcal{I}(\phi)=\frac{2I_k\cos^2(\phi_k-\phi_t)\sin(\phi_k-\phi_t)\sin(\phi-\phi_t)}{[\sin(\phi_k-\phi_t)\cos(\phi-\phi_t)]^2+[\cos(\phi_k-\phi_t)\sin(\phi-\phi_t)]^2} \tag{11}$$

Figure 1b illustrates the $k=3$ case, the solid segment being relevant, and $\phi_t=\pi+\tan^{-1}(d\delta/dx)$.

Results and Discussion

Typical results and comparisons with *M.E.* are shown in Figs. 2-4 for a $\theta_w=0.61$-rad wedge at $M_\infty=28.5$ and 35.5 and an altitude of 60 km. Lengths (x,δ) are in units of wedge surface length L, say, and radiative flux and intensity are in units of σT_s^4, the blackbody flux for conditions immediately behind the shock at the leading edge. For $M_\infty=28.5$, $T_s=2\times10^4$K,

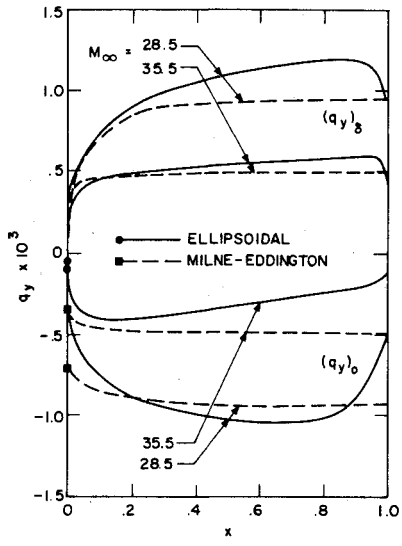

Fig. 3 Flux distributions to wedge surface and stream, in surface normal direction, $\theta_w = 0.61$ rad, $(M_\infty, \tau_L, Bo) = (28.5, 0.62, 0.027)$ and $(35.5, 5.42, 0.0092)$.

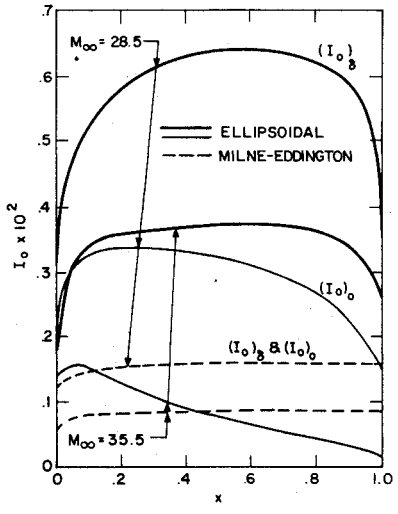

Fig. 4 Intensity distributions along surface and shock, $\theta_w = 0.61$ rad, $(M_\infty \tau_L, B_0) = (28.5, 0.62, 0.027)$ and $(35.5, 5.42, 0.0092)$.

$\alpha_s = 0.355$/m, and $\sigma T_s^4 = 9 \times 10^9$ W/m^2. Boltzmann and Bouguer numbers are defined as $Bo = (\rho u h/\sigma T^4)_s$ and $\tau_L = \alpha_s L$, with $L = 1.75$ m for an assumed 1-m base height. All numerical values correspond to Ref. 1 to enable comparison. For these conditions, emission is appreciably larger than absorption and the significant differences in I_0 for *M.E.* and ellipsoidal modeling imply negligible differences in the corresponding strongly coupled fluid field.

The surface parallel flux q_{x_0} is indicative of the modeling importance (Fig. 2). This is consistent with the pure radiation field studies[4,5] that pointed out the errors in *M.E.* for flux components not constrained by the boundary condition. *M.E.* failure is clear, in fact, from the $|q_x| \approx 7I_0$ result (see Fig. 4) at the nose, whereas moment definitions require $|q_x| \leq I_0$. The comparison is not as poor at the downstream boundary where the matching of average (for the integral method) I_0 and q_x are imposed.

The normal flux component, q_{y_0}, provides surface heating (Fig. 3). Increasing M_∞ (or wedge angle[5]) leads to stronger shocks and the increasingly dominant radiation over convection (i.e., decreasing *Bo*) implies significant radiative cooling over a lesser distance. This effect tends to offset the increased absorption at the nose and results in a moderate increase in the actual (longitudinal) optical depth ($\int \alpha dx$) despite a considerable increase in the nominal $\alpha_s L$. Near the base, the transverse optical depth actually decreases. The influence of earlier cooling is absent from *M.E.* The overprediction of *M.E.* nose heating by a factor of six is especially important, and is associated with the boundary condition $q_{y_0} = -I_0/\sqrt{3}$, even in situations where the intensity concentration is in the xz plane. The areas between the q_{y_0} and q_{y_δ} distributions in Fig. 3 are a measure of the total fluid energy loss, and the reasonable agreement between *M.E.* and ellipsoidal methods is a consequence of the emission dominance.

Differences in I_0 fields (Fig. 4) between the methods indicate the appreciably different flowfields that must be expected with increasing absorption. The essentially constant I_0 distributions for *M.E.* are even more striking than the disagreement in magnitude. This behavior may be traced to the *M.E.* flux constraint $dI_0/dy \sim q_y$ which, for geometrically thin layers, implies large q_y for any significant I_0 change. However, for emission dominance, the integrated q_y must be accurate, limiting I_0 variations normal to the surface. The implications extend beyond a poor absorption representation to imposing virtually identical outward fluxes at both surface and shock, since the *M.E.* normal flux is related there to the local I_0. This is apparent in the *M.E.* curves in Fig. 3, where half of the radiated energy issues from each lateral boundary.

Although reabsorption may be relatively small everywhere ($M_\infty = 28.5$), in some situations ($M_\infty = 35.5$) reabsorption and emissions are comparable near the base (for either *M.E.* or ellipsoidal). Physically, this tends to diminish the surface-directed radiation by reabsorption and subsequent isotropic re-emission. The net effect is that more than half of the energy is radiated out through the shock, as made clear by the ellipsoidal results in Fig. 3. Thus, even in instances of overall insignificant reabsorption, the modeling is of some importance to the distributed absorption influence.

References

[1] Gibeling, H. J. and Baron, J. R., "Minimum Radiative Transfer Geometries," *Journal of Computers and Fluids*, Vol. 1, Jan. 1973, pp. 379-398.

[2] Jischke, M., "Radiation Coupled Wedge Flows," *AIAA Journal*, Vol. 4, July 1966, pp. 1300-1302.

[3] Olfe, D. B., "Radiative Cooling in Transparent Shock Layers of Wedges and Cones," *AIAA Journal*, Vol. 4, Oct. 1966, pp. 1734-1740.

[4] Elgin, J. B. and Baron, J. R., "A Variable Closure Differential Approximation for Anisotropic Radiation," *Journal of Quantitative Spectroscopy and Radiative Transfer*, Vol. 16, Oct. 1976, pp. 805-818.

[5] Elgin, J. B., "Anisotropic Radiative Transfer in Gas Dynamics," Ph.D. Thesis, Feb. 1976, Massachusetts Institute of Technology, Cambridge, Mass.; also, TR-75-1564, Air Force Office of Scientific Research, 1975.

[6] Vincenti, W. G. and Kruger, C. H., *Introduction to Physical Gas Dynamics*, Wiley, New York, 1965, Chap. 12.

[7] Zeldovich, Y. B. and Raizer, Y. D., *Physics of Shock Waves and High Temperature Hydrodynamic Phenomena*, Vol. 1, Academic Press, New York, 1967, Chap. 2.

Radiative Ablation of Melting Solids

Anant Prasad* and S.N. Sinha†
Regional Institute of Technology, Jamshedpur, India

Nomenclature

c	= heat capacity per unit volume of the solid
H	= heat flow vector
k	= thermal conductivity of the solid
L	= latent heat of the solid
$q_1(t)$	= unknown surface temperature
$q_2(t)$	= melting distance
t	= time

Received April 28, 1976; revision received July 6, 1976.
Index categories: Heat Conduction; Material Ablation.
*Assistant Professor, Department of Mechanical Engineering.
†Lecturer, Department of Metallurgical Engineering.